ELSEVIER

Marine Geology 195 (2003) 223–236

MARINE GEOLOGY
INTERNATIONAL JOURNAL OF MARINE GEOLOGY, GEOCHEMISTRY AND GEOPHYSICS

www.elsevier.com/locate/margeo

Numerical modelling of mud volcanoes and their flows using constraints from the Gulf of Cadiz

Bramley J. Murton *, Juliet Biggs [1]

Southampton Oceanography Centre, Empress Dock, Southampton SO14 3ZH, UK

Received 15 June 2001; accepted 5 November 2002

Abstract

It is estimated that the total number of submarine mud volcanoes is between 1000 and 100 000. Because many are associated with greenhouse gases, such as methane, it is argued that the global flux of these gases to the atmosphere from the world's terrestrial and submarine mud volcanoes is highly significant. Clues to the processes forming submarine mud volcanoes can be found in variations to their height, shape, surface morphology, physical properties and internal structure. A model of isostatic compensation between the mud column and the sediment overlying the mud source is used to predict a depth to the mud reservoir beneath mud volcanoes. Once erupted, the general behaviour of an individual mud flow can be described and predicted using a viscous gravity-current model. The model shows that conical-shaped mud volcanoes comprise multiple, superimposed radial flows in which the thickness, eruption rate and speed of individual mud flows strongly depends on the viscosity, density and over-pressure of the erupted mud. Using these parameters, the model predicts the lowermost flows will be the oldest, thickest and have the greatest length of run-out while the uppermost flows will be the youngest, thinnest and shortest. This model is in contrast to more traditional models of stratiform mud volcano construction in which younger flows progressively bury older ones and travel furthest from the summit. Applying the model to the two mud volcanoes studied in the Gulf of Cadiz, quantitative estimates are derived for the depths to mud sources, exit and flow velocities, eruption duration and volume fluxes, flow thickness and conduit radii. For example, with an average kinematic viscosity of 1.5 $m^2\ s^{-1}$ for the erupted mud, a density of 1.8×10^3 kg m^{-3} and a thickness for the youngest flows of about 0.5 m, the model predicts a lowermost flow thickness of 3.6 m, an average eruption duration of 7 h and a conduit radius of about 9 m. To construct a conical-shaped mud volcano of 260 m height, similar to those studied in the Gulf of Cadiz, is estimated to require a mud source at 4.6 km depth and a total of at least 100 individually erupted flows.

Keywords: mud volcanoes; numerical modelling; Gulf of Cadiz

1. Introduction

Submarine mud volcanoes, ranging in size between 50 cm and 800 m high, occur world-wide on continental shelves, slopes and in the abyssal parts of inland seas. It is estimated that total number of submarine mud volcanoes is between

[1] Present address: Department of Earth Sciences, University of Cambridge, Downing Street, Cambridge CB2 3EA, UK.
* Corresponding author. Fax: +44-1703-596554.
E-mail addresses: b.murton@soc.soton.ac.uk (B.J. Murton), bjm@soc.soton.ac.uk (B.J. Murton).

0025-3227/02/$ – see front matter © 2002 Elsevier Science B.V. All rights reserved.
doi:10.1016/S0025-3227(02)00690-4

1000 and 100 000 (Milkov, 2000). Two major processes are identified as forming mud volcanoes: high sedimentation rates and lateral tectonic compression, both causing over-pressure of a mobile mud source at depth within the sediment column. Of these processes, two basic mechanisms are thought to further account for the actual eruption of mud on the seafloor: the unroofing and exposure of upward-migrating shale or mud diapirs, and the rise of mobile sediments along crustal pathways that typically include fault planes. In both cases, subsurface fluid migration is considered critical to the formation of mud volcanoes (Milkov, 2000).

Some studies (e.g. from the Barbados accretionary complex) have linked the morphology of submarine mud volcanoes to different development stages and processes of mud liquefaction (Limonov et al., 1997; Lance et al., 1998). Conical-shaped mud volcanoes ('mud-mounds' or *gryphons*), which do not have any central summit 'mud lakes' (or *salses*), are formed by the expulsion of plastic mud breccia in concentric radial flows. In contrast, shearing with the feeder conduit liquefies the mud leading to the formation of flat-top mud volcanoes (*mud-pies*) with central 'mud lakes' and elongated, radial mud-flow tongues. In both types, the mud is found to have a plastic behaviour in which its yield strength decreases with increasing porosity. Thixotropy is associated with high porosity (e.g. more than 70%), which is often related to the dissociation of gas hydrate (Lance et al., 1998).

Often, mud volcanoes are associated with methane fluxes, either as free gas or, depending on ambient temperature and pressure conditions, as gas hydrate (Limonov et al., 1997; Cronin et al., 1997). On this basis, Hovland et al. (1997) argue that the global flux of methane to the atmosphere from the world's terrestrial and submarine mud volcanoes is 'highly significant'.

The relative difficulty in studying submarine mud volcanoes, compared with their terrestrial counterparts, leaves substantial gaps in our knowledge about their modes of formation, the duration and frequency of eruptions and the fluxes of mud and volatile phases from the subsurface. This paper introduces a simple numerical model for the formation of conical-shaped mud volcanoes. The model, which is based on sonar data and gravity cores from mud volcanoes in the Gulf of Cadiz, yields estimates for the volume and duration of eruptions for two individual mud volcanoes. Although the model is directly applicable to what are described as the 'conical' types of mud volcano, it is also a useful way of identifying the first-order parameters that control mud volcano formation in general and of estimating the fluxes of fluids from the subsurface.

2. Data

The data used here are from a study of the Gulf of Cadiz, made during cruises TTR-9 and TTR-10 of the R/V *Professor Logachev* (Fig. 1) and reported by J.M. Gardner and others in Kenyon et al. (2000). Specifically, this study focuses on the structure and evolution of two submarine mud volcanoes (named Yuma and Ginsburg in Akhmanov et al., 2000) located in the Gulf of Cadiz.

2.1. Geological setting

Interaction between the Iberian and African plates has resulted in a complex sedimentary and tectonic history for the Gulf of Cadiz and adjacent continental margins, in the eastern North Atlantic. This history includes several episodes of extension and compression since the Triassic (Wilson et al., 1989; Dewey et al., 1989; Srivastava et al., 1990; Maldonado et al., 1999). During the Late Tortonian, westward movement of the Gibraltar Arc caused the Gulf of Cadiz to form a forearc basin (Maldonado and Comas, 1992). As a result, olistostrome emplacement occurred forming accretionary wedge-type deposition and later deformation (Blankenship, 1992; Flynch et al., 1996; Maldonado and Somoza, 1997; Maldonado et al., 1999). In the Early Pliocene, extensional collapse of the basin, coupled with mud and shale diapirism, influenced sediment deposition (Rodero et al., 1999; Maldonado et al., 1999).

During research cruise TTR-9, three regions of

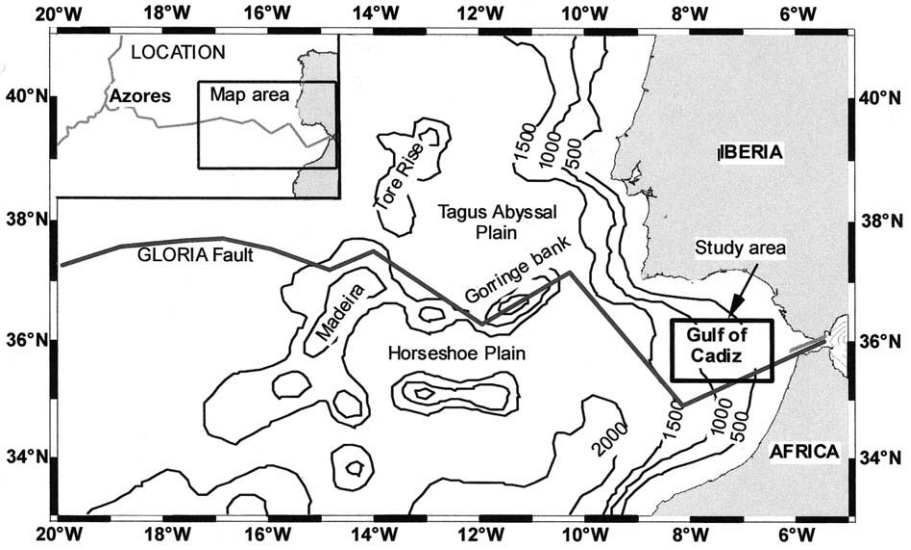

Fig. 1. Schematic location and bathymetry chart (contours at 1000-m intervals) of the study area in the Gulf of Cadiz, eastern North Atlantic.

mud volcanism were identified in the Gulf of Cadiz region: the Western Moroccan Field, Middle Moroccan Field and Eastern Moroccan Field (Kenyon et al., 2000; Gardner, 2001). Here, the focus is on results from two mud volcanoes located in the Middle Moroccan Field. These were initially identified from 12-kHz surface-towed side-scan sonar records and subsequently confirmed using deep-tow 30-kHz side-scan sonar, photography, grab samples and gravity cores (Kenyon et al., 2000). Single-channel seismic data reveal that mud volcanism post-dates sedimentation and is probably Holocene to Recent in age (Kenyon et al., 2000).

The two mud volcanoes, Yuma and Ginsburg, lie along an approximately NNW–SSE-oriented line. Their centres are separated by ~7 km and both volcanoes are roughly 4 km in diameter, with a vertical relief of about 200 m (Fig. 2a,b). The northernmost mud volcano (Yuma) consists of a large, gently domed summit upon which a smaller dome is located. Both domes have concentric ring structures surrounding their centres. These ring structures have amplitudes of over 1 m and comprise a series of circular ridges and troughs. Gravity cores recovered from the summit of the main dome reveal a thin layer of pelagic clay and marl (less than 50 cm thick) overlying a thicker sequence of mud breccia, while pelagic sediments are absent from the summit of the smaller dome (Kenyon et al., 2000). The southernmost mud volcano (Ginsburg) is of similar proportions to Yuma, but comprises only one conical dome. Like Yuma, the Ginsburg dome is also surrounded by a series of concentric rings of ridges and troughs. Gravity cores from the summit of the Ginsburg volcano recovered a thin layer of pelagic clay and marl overlying mud breccia (Kenyon et al., 2000). Both mud volcanoes have convex flanks with maximum gradients of about 1:10 and are located within moat-like depressions, 80–90 m deep, that enclose their outer margins. The origin of the moats is probably subsidence, resulting from the eruption of mud from some depth below the volcano, and may therefore be similar to the processes of caldera formation.

Density measurements made on mud breccia immediately after recovery from the summits of both mud volcanoes yield a range from 2.0 to 1.75×10^3 kg m^{-3}. Viscosity measurements were made for the mud breccia using a capillary method. This involved forcing a known volume of recently collected mud breccia through a tube of known diameter under constant pressure. Differ-

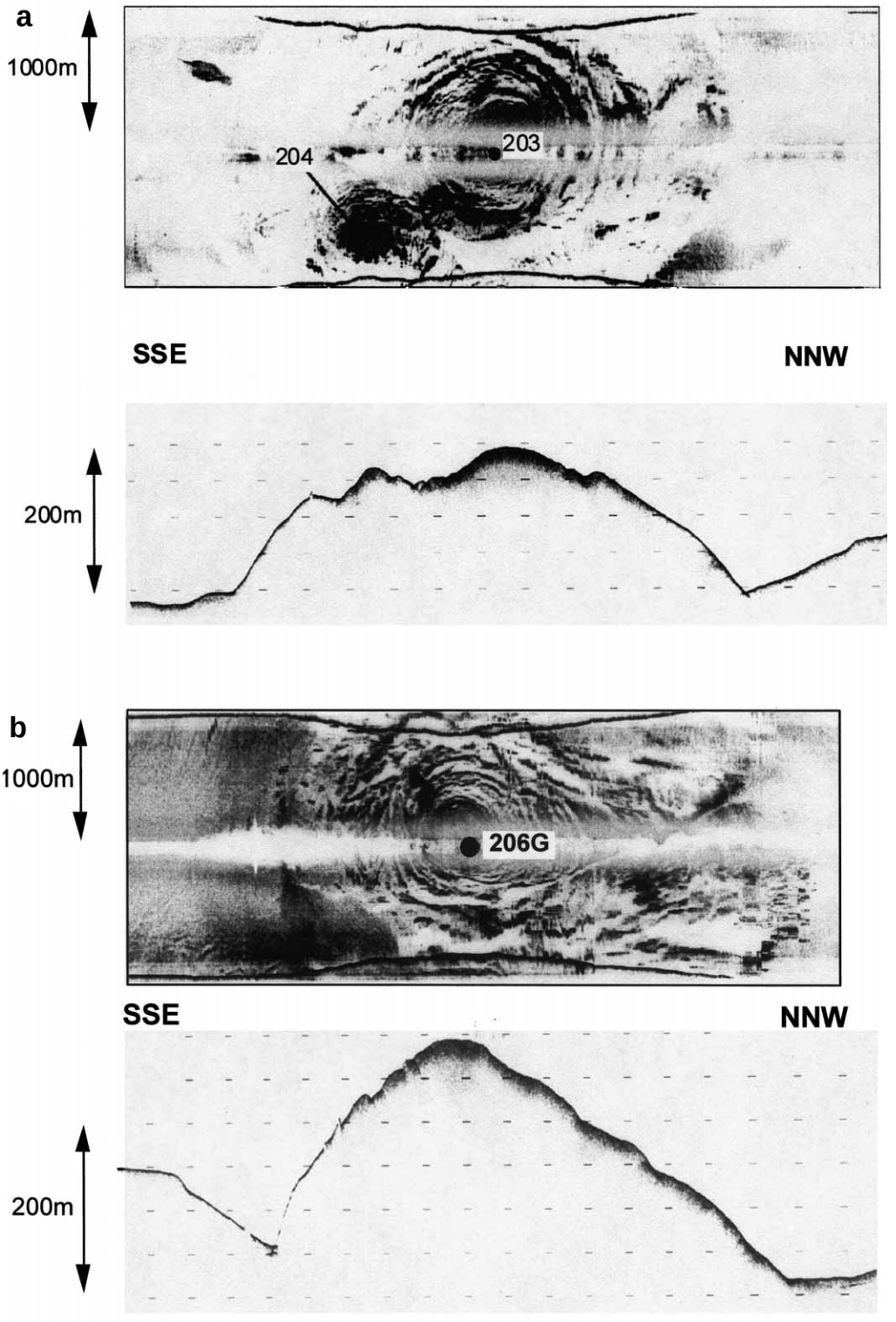
a
1000m
204
203
SSE
NNW
200m
b
1000m
206G
SSE
NNW
200m

ent volumes were tested and repeated several times. The tests confirmed a plastic behaviour for the mud breccia, recognised for mud volcanoes elsewhere (Lance et al., 1998), and yielded a range in kinematic viscosity (ν) of 0.9–3 $m^2\ s^{-1}$. Yield strength measurements, made by Gardner (personal communication), gave values of about 5×10^3 N m^{-2} and 8×10^3 N m^{-2} (i.e. 5 and 8 kPa) for mud breccia recovered from Ginsburg and Yuma respectively. Although no free gas was evident in the mud breccia, in situ gas hydrate crystals were recovered from approximately 1.5 m below the summit of Yuma (Kenyon et al., 2000). The presence of free gas, variable fluid content and lithoclasts (up to several centimetres in diameter) within the mud breccia affect its viscosity and density. For the purposes of simplifying the modelling, an average density of 1.8×10^3kg m^{-3} and homogeneous kinematic viscosity of 1.5 $m^2\ s^{-1}$ has been assumed for the mud breccia. Although the accuracy of these parameters is not imperative here, since their variation alters only slightly the details of the results and not the general form of the model, further studies should seek to determine their values more accurately.

3. Results and discussion

3.1. An isostatic model

In the following section a simple buoyancy model is developed to relate the maximum height of a mud volcano to the thickness of its overburden. Such a buoyancy-driven, or isostatic equilibrium, concept is not new and has been applied to igneous volcanic provinces in the past (Vogt, 1974; Smith and Cann, 1993). Its application to mud volcanoes, however, is believed to be new and reveals important constraints on the depth of the source of the mud breccia within the sediment pile. These constraints allow, among other things, comparison with seismically determined depths to the mud breccia source as well as indications of the stratigraphic depth of origin for lithoclasts contained within the mud breccia, described by Sadekov and Ovsyannikov (2000).

All mud volcanoes require, at some depth within the sediment pile beneath them, a reservoir or source of mobile mud. Once a conduit has been opened to the surface, the mud is driven upwards by over-pressure, caused mainly by the density and weight of the overburden. Mineral dehydration reactions, as well as biogenic and petrogenic gas generation, will further contribute to the over-pressure by reducing the density of the fluid mud. Assuming over-pressure is largely a function of overburden, the maximum height a mud volcano can achieve is a balance between the weight of the overburden and the weight of a mud column that extends from the top of the volcano to the mud reservoir. For mud volcanoes that have achieved their maximum height, it can be assumed that this reservoir is located at a depth of isostatic compensation. For example, the pressure at the base of the column of mud breccia connecting the reservoir to the top of the volcano, plus the overlying seawater, must equal the pressure at the base of the sediment pile plus the overlying seawater (see Fig. 3).

Critical parameters in this calculation are the

Fig. 2. (a) 30-kHz side-scan sonar image (top) and sub-bottom profile (bottom) of the mud volcano Yuma (dark tones indicate high acoustic back-scatter), shown with the same horizontal scale. Core 203 recovered mud breccia with a ~25-cm cap of pelagic marl while core 204 recovered mud breccia without any pelagic sediment cap (after Gardner, 2000). Note the concentric ring-like structures that are centred on the main summit with the small dome to its left. The profile also shows the summit of the volcano surrounded by a moat, indicating partial subsidence of the top of the main dome. (b) 30-kHz side-scan sonar image (top) and sub-bottom profile (bottom) of the Ginsburg mud volcano, shown at the same horizontal scale. The summit core 206G recovered mud breccia with a ~50-cm cap of pelagic marl and mud (after Kenyon et al., 2000). Note, as for Yuma, the concentric ring-like structures that are centred on the main summit of the dome. Also note the elongated flow-like structure on the NNW flank. Unlike Ginsburg, which is more conical, the profile of Yuma reveals depressions in the summit indicating there has been some significant post-eruptive subsidence. The small cone on the SSE side of the summit has been active more recently than the apex of the volcano, indicating parasitic cone growth.

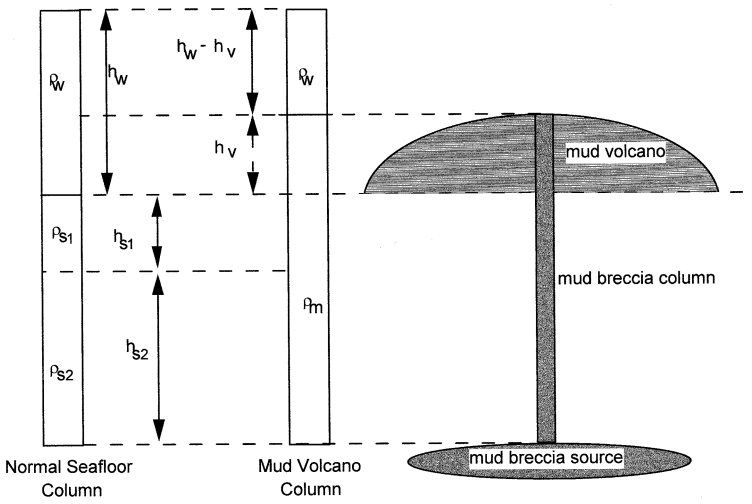

Fig. 3. Schematic figure showing the main elements of the isostatic model, comprising the columns of mud breccia, the mud volcano conduit, and a two-layered sediment column model, in which: ρ_m = density of mud $\approx 1.8\times10^3$ kg m^{-3}; ρ_w = density of seawater $\approx 1\times10^3$ kg m^{-3}; ρ_{s1} = density of uppermost sediment $\approx 1.65\times10^3$ kg m^{-3}; ρ_{s2} = density of lowermost sediment $\approx 1.9\times10^3$ kg m^{-3}; h_{s1} = height of uppermost sediment column (i.e. $\sim$1 km); h_{s2} = height of lower sediment column above depth of isostatic compensation (i.e. depth of mud reservoir – to be determined); h_w = height of water column above surrounding seafloor; h_v = height of volcano surrounding seafloor $\sim$266 m (Ginsburg).

density structure of the mud breccia and the sediment pile through which the mud is erupted. Due to the lack of subsurface well data in the vicinity of the Ginsburg and Yuma mud volcanoes, a compilation of sediment density values from accretionary sedimentary sequences is used, determined from several ODP sites (Mascle et al., 1988; Shipley et al., 1995; Karig, 1986; WWW data resources; http://www.ldeo.columbia.edu/BRG/ODP/DATABASE). The sediment density increases from 1.3×10^3 kg m^{-3} at the surface to approximately 2×10^3 kg m^{-3} below a depth of 2000 m subsurface (Fig. 4). For the purposes of this contribution, a simplified two-layer sediment density model is used. The uppermost 1 km has an average density of 1.65×10^3 kg m^{-3} and sediment deeper than 1 km has an average density of 1.9×10^3 kg m^{-3}.

Gravity cores from the summits of both Yuma and Ginsburg mud volcanoes, taken during cruises TTR-9 and TTR-10, found a veneer of pelagic sediment overlying the mud breccia (Kenyon et al., 2000). This indicates that the mud volcanoes are presently inactive and have probably reached their maximum height. Assuming this to be the case, an expression for the thickness of the sediment column above a mud breccia reservoir can be derived by equating the pressures at the bottom of the sediment column to that at the base of a mud volcano column (Fig. 3).

Pressure under normal seafloor column:

$$h_{sa}\rho_{s1} + h_{s2}\rho_{s2} + h_w\rho_w \quad (1)$$

Pressure under mud volcano column:

$$(h_s + h_v)\rho_m + (h_w - h_v)\rho_w \quad (2)$$

Solving for the unknown thickness of the lower sediment column, h_{s2}, yields:

$$h_{s2} = [h_v(\rho_m - \rho_w) - h_{s1}(\rho_{s1} - \rho_m)]/(\rho_{s2} - \rho_m) \quad (3)$$

Substituting the values for density and volcano height for Yuma (200 m) and Ginsburg (266 m) into Eq. 3 yields a total depth to the mud breccia sources of 4600 m and 4100 m respectively. These results are susceptible to variations in the estimates of the density of the sediment column and mud breccia. Increasing the sediment column density, or reducing the mud breccia density, reduces the calculated depth to the mud breccia source. For example, the density of the mud breccia

may be affected by variations in its volatile or water content. The presence of 10% by volume of a hydrous phase of dissolved gas and water, with a density of 1×10^3 kg m^{-3}, will reduce the mud breccia density by 4%. This in turn will decrease the estimated depth to the mud source by 12%.

A consequence of the isostatic model is a prediction for the type and location of future eruptions for a mud volcano that has reached its maximum height. Unless the mud volcano subsides, future eruptions can only occur if either the mud breccia density decreases, if there is an increase in its over-pressure or overburden, or if the eruption occurs from the flanks of the volcano. This prediction is supported by observations of the Yuma mud volcano. Its bathymetric profile (Fig. 2a) shows that the SE side of the main summit is concave, within which a smaller mound is located. This we interpret as evidence for subsidence of the summit. Although cores indicate pelagic drape for the main summit, and hence evidence that eruptions have ceased there, the smaller mound on the top of Yuma does not have pelagic drape. This is interpreted by us as evidence for active parasitic cone growth following subsidence, as predicted by the model. The Ginsburg mud volcano does not have any obvious concave features or parasitic cones and summit cores show a pelagic sediment veneer. Hence, although it has probably reached its maximum height, unlike Yuma, Ginsburg probably has not experienced significant summit subsidence and hence there is no cause for reactivation of mud eruptions. Furthermore, assuming both volcanoes have similar depths to their fluid mud reservoirs, the model predicts that the volcano Yuma, which is 66 m lower than Ginsburg, should be the more active, which appears to be the case.

3.2. An eruption model

Here, a simple model describing the processes controlling the eruption, spread and thickness of individual mud breccia flows is developed. This model uses the theory describing gravity-driven viscous currents to predict both the shape and internal structure of individual mud volcanoes.

3.2.1. Input parameters

The motion of a fluid, spreading across a solid surface, is determined by the balance of the forces

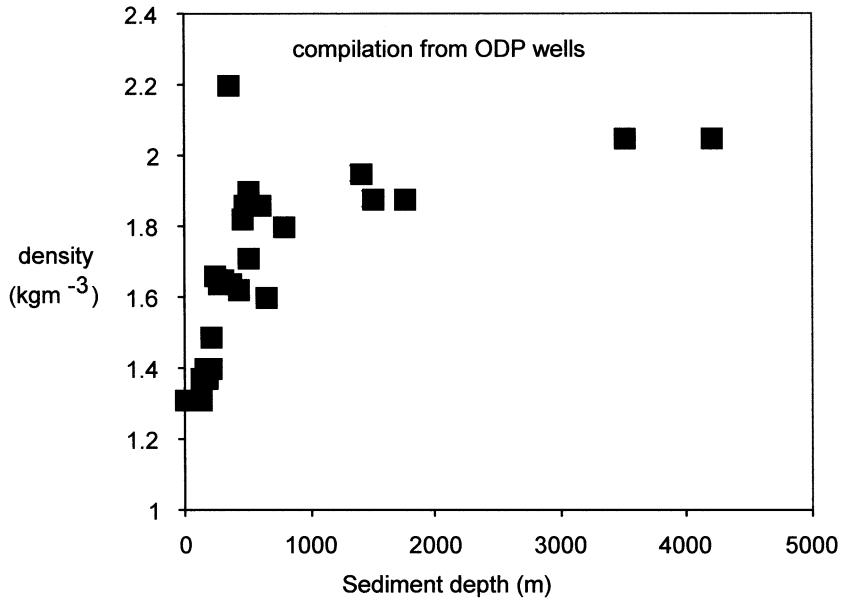

Fig. 4. Compilation of clastic sediment densities from ODP holes in accretionary complexes including the Barbados Forearc Wedge (see references in text). The sediment column increases in density from 1.3 to 1.9 kg m^{-3} over the uppermost 1 km.

acting upon it. These various forces are either directed towards accelerating or resisting its motion. In the case of erupting mud flows, the major force of acceleration is gravity, resulting from density differences between the flow and its surrounding fluid (in this case mud and seawater). The retarding forces are the flow's inertia, viscosity and yield strength. Of these, viscosity dominates the majority of the flow's eruption history with inertia important only at the beginning and yield strength at the end.

The role of gas and fluids in reducing the density of the mud breccia has already been mentioned. By analogy with magmatic volcanoes, an increased content of such volatiles will also reduce its viscosity. However, unlike magmatic lavas that can degas as they erupt, the presence of stable gas hydrates on mud breccia recovered from the summits of the two submarine mud volcanoes considered here provides little opportunity for degassing. Therefore, in the absence of evidence to the contrary, we have assumed the erupting mud flows have constant viscosity. The measurements of the viscosity of the mud breccia include its yield strength. However, the yield strength of the mud breccia only becomes dominant at the outer boundary conditions of the flow (i.e. when the flow velocity tends towards zero), when gravity-induced stresses within the flow tend towards the value of the shear strength. Yet the evidence that the mud flows support an elevated volcano structure implies an increase in shear strength with time, possibly by dewatering of flows during increasing burial beneath subsequent deposits.

3.2.2. *Viscous-gravity currents: a numerical analogue for mud eruption*

To construct this simple model, mud volcanoes are assumed to erupt with a constant volume flux (Q), from a conduit with a constant diameter, onto a horizontal base. The volume flux is controlled by the buoyancy of the mud and its kinematic viscosity (ν). This produces a radially symmetric, laminar flow, whose properties are uniform at a given radius and time. In the case of a gravity-driven current, such as that formed during eruption of a mud volcano, the erupted material (with a density ρ) is denser that the ambient fluid (with a density ρ_a, where $\rho > \rho_a$). Therefore, the erupted mud spreads and flows across the seafloor. The flow is driven by its density contrast with seawater, which is usually expressed in terms of 'reduced gravity', g', where

$$g' = g\Delta\rho/\rho \quad \text{where}: \ (\Delta\rho = \rho - \rho_a) \tag{4}$$

Conversely, the flow is retarded by viscous drag (its kinematic viscosity, ν) and also by its inertia, provided the discharge Froude number is subcritical, i.e.:

$$U_i/(g'h_i)^{1/2} < 1 \tag{5}$$

where U_i is the horizontal inflow velocity and h_i is the depth or thickness of the initial flow.

Three main forces act on a viscous gravity flow: buoyancy, viscosity and inertia (Didden and Maxworthy, 1982). The magnitude of these forces varies as a function of time (t). During its initiation, inertia is the dominant retarding force acting on a gravity current. The duration of this initial period (t_i) is given by:

$$t_i = (Q/g'\nu)^{1/2} \tag{6}$$

The duration of the initial condition (t_i) can be quantified, providing there is an estimate of the volume flux of the mud breccia as it initially erupts. To estimate this, the flow through the volcano's conduit is treated as forced viscous fluid flow through a capillary. Assuming the driving force is a result of the pressure difference between the bottom of the mud breccia column and the bottom of the sediment column and the retarding forces are dominated by viscous drag, Eq. 7 can be applied to describe the volume flow (Q) through the conduit:

$$Q = P\pi r^4/8l\eta \tag{7}$$

where P is the driving pressure, l is the length of the conduit (in this case the height of the initial mud breccia column), r is the average radius of the conduit, and η is the dynamic viscosity of the mud breccia.

The isostatic model, already used to estimate the depth of the mud reservoir, can also be used to predict the driving pressure (P) for an immature mud volcano. Initially, the volcano is fed by a source of mud at depth within the sediment

column. At this stage, the volcano has not yet formed any elevated structure at the surface. Thus the driving force is approximately equivalent to the pressure difference between the base of a column of mud breccia and the column of sediment, both equivalent in height to the depth of the mud source, as described by Eqs. 1 and 2. Using the Ginsburg mud volcano as an example, with an estimated eruptive column length of 4600 m, the resulting driving pressure is 2.12×10^6 N m^{-2} (e.g. 2.12×10^3 kPa).

Although none of the data for Ginsburg give a clear indication of the radius of the conduit, its bathymetric profile shows a gently domed top with a radius of 100 m providing us with a maximum dimension. Taking the dynamic viscosity, η, measured from the mud breccia as 3000 kg m^{-1} and a range of possible conduit radii yields the flow rate (Q) (from Eq. 7) and the duration of the inertia-dominated flow (t_i) (from Eq. 6); e.g.:

If $r = 100$ m, then $Q = 6\times10^6$ m^3 s^{-1}, $t_i = 950$ s
If $r = 10$ m, then $Q = 6\times10^2$ m^3 s^{-1}, $t_i = 9.5$ s
If $r = 1$ m, then $Q = 0.06$ m^3 s^{-1}, $t_i = 0.09$ s

Thus the duration of inertial retardation of mud flow eruption is unlikely to be significant for those flows with an eruption history lasting several hours. However, because there are no direct measurements of flow velocity, at this stage it can only be assumed that inertial retardation is insignificant. This assumption is revisited in a later section, where it is argued that flow duration is of the order of several hours.

For the period following inertial retardation, (i.e. when $t > t_i$), the dominant retarding force acting on an individual mud flow is viscous drag. In this regime, the thickness at the eruptive centre, h_0, and the radius of the flow, R, can be described by the following expressions (after Didden and Maxworthy, 1982):

$$R \approx (g' Q^3/\nu)^{1/8} t^{1/2} \quad (8)$$

$$h_0 \approx (\nu Q/g')^{1/4} \quad (9)$$

where the symbol $\approx$ denotes only approximate accuracy. Differentiating the radius with respect to time, while assuming a constant volume flux, yields an expression for the velocity of the flow front, U:

$$U \approx (g' Q^3/\nu)^{1/8} t^{-1/2} \quad (10)$$

Eqs. 8 and 9 can be used to estimate the thickness and radius of flows during individual eruptions. Cores recovered from the mud volcanoes provide evidence for several layers of erupted mud, indicating a history of activity involving discrete episodes of eruption (Kenyon et al., 2000). Eq. 8 shows that the run-out radius of a flow increases with the square root of time while Eq. 9 shows that the central thickness of an individual mud flow is independent of time. Hence, assuming a constant volume flux during eruption, the velocity of a flow front (derived from Eq. 10) decreases, maintaining a constant flow thickness. This shows that the thickness of a flow at any given run-out radius is independent of time and equal to the thickness of the flow at its centre. The product of such a model is a roughly cylindrical flow that spreads radially outwards from its central point of eruption.

During construction of a mud volcano, subsequent eruptions are superimposed upon preceding ones, building a layered structure. The increasing height of the volcano reduces the driving pressure for each new eruption, which in turn reduces the volume flux, resulting in subsequent flows being thinner and spreading more slowly than their predecessor (i.e. from Eqs. 8, 9 and 10). Because the surface of each flow is horizontal, subsequent new flows are extruded in an identical way to their predecessors. This model predicts an *idealised* structure for conical mud volcanoes as one composed of multiple, laminar flows, stacked vertically, each decreasing in thickness and radius

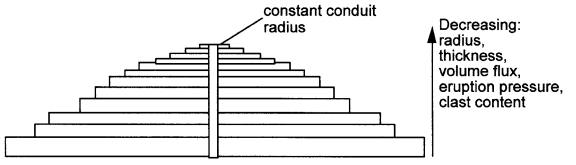

Fig. 5. Schematic cross-section (not to scale) showing elements of a vertically stacked model of mud volcano formation, with a central conduit of constant diameter, in which the thickness and radius of superimposed, cylindrical mud flows both decrease with increasing volcano height.

with height (Fig. 5). However, should the duration of a new flow exceed its predecessor's it will reach the edge of the underlying flow and cascade down the flank of the volcano. Such over-spills have a distinctive appearance on side-scan sonar records, forming elongated radial flows. A possible example of this is seen on the NW flank of Ginsburg (Fig. 2).

3.3. Applications to Ginsburg and Yuma

To determine better the idealised evolution of a mud volcano, as described by the model, constraints on the volume flux (Q) during mud eruptions are needed. As there are no direct observations of these, values of Q must be inferred from observations such as flow thickness (e.g. by substituting these parameters into Eq. 9). Gravity cores from the summit of the mud volcanoes recovered several erupted mud units with an average thickness of 0.5 m (Kenyon et al., 2000). Eq. 9 yields an estimated volume flux of 0.18 m^3 s^{-1} from a flow thickness of 0.5 m. Such a low value is expected since these flows were recovered from the summit of the volcano (i.e. near its maximum potential height). An estimate for the conduit radius can derived from Eq. 7 by substituting a reduced value for the driving pressure (P) and an extended length of the conduit (l), consistent with eruption at the summit. Using the derived value for the volume flux for the 0.5 m thick flows at the summit, P at 1% of its value at the base of the volcano and l equal to h_v+h_s (i.e. 4600+266 m), Eq. 7 yields a conduit radius of 9.4 m. Note that Eq. 7, when solved for the radius of the conduit, yields a result that is dependent only on the 1/4 power of the products of viscosity, conduit length, volume flux, and driving pressure, and is therefore relatively insensitive to uncertainties in these parameters. For example, the estimated radius varies by only 16% for a 100% uncertainty in the volume flux or driving pressure.

Assuming the conduit radius is of similar dimensions throughout the height of the volcano, then the volume flux during each subsequent eruption decreases linearly with increasing height. This in turn results in decreasing flow thickness with height and, for a similar duration of eruption, decreasing flow radii (Fig. 6). With the superposition of subsequent flows, the volcano will evolve a convex, dome-like profile (Fig. 7) similar to the profiles presented by Yuma and Ginsburg.

Because we do not known the duration of the periods of inactivity, it is impossible to estimate the time for the construction of mud volcanoes like Yuma or Ginsburg. However, the model can be used to estimate the duration of individual flow events. For example, assuming constant volume flux for its duration, Eq. 7 yields a volume flux for the initial eruptions forming the base of the volcano of about 472 m^3 s^{-1} (i.e. with a conduit radius of 9.4 m). Eq. 9 then yields a thickness for this flow of 3.5 m. Side-scan images of the volcanoes show basal radii of about 2 km. From Eq. 8, substituting this value for the flow radius (R) and solving for time (t) yields a duration for the run-out of the flow of about 7 h. The construction of Ginsburg requires an estimated 100 individual flows, ranging in thickness from 3.5 m at its base to 0.5 m at its summit. The estimate of the number of flows will increase if there is post-eruption subsidence, flattening or spreading of the volcano.

3.3.1. On the origin of the concentric ring structures

Both of the side-scan sonar images of Yuma and Ginsburg show closely spaced concentric rings about the centre of the two mud volcanoes (Gardner, 2001). Although these structures can be interpreted as subsidence features, the concentric rings are observed for both Yuma (which has arguably experienced some component of summit subsidence) and Ginsburg (for which there is less evidence from the bathymetric profile for summit subsidence). An alternative explanation for the origin of the rings is a periodic fluctuation in volume flux during the formation of the mud volcano. In this case, each ring would represent an individual, near-circular, mud flow front. This interpretation is consistent with the model, which predicts radial run-out and superposition of circular mud flows. Furthermore, the outermost and oldest flow fronts are more likely to be partially obscured by post-eruption pelagic sedimentation

and viscous slumping than the younger, innermost rings. These predictions are supported by side-scan sonar images of the structures which show the rings toward the centre are more clearly defined than the outer rings (i.e. which appear increasingly obscured and disturbed).

It is possible to explore further the origin of the concentric ring structures by comparing their amplitude with the predicted thickness of flows at the position occupied by the rings on the flanks of the volcanoes. If the rings are tectonic structures, then there is no reason why they should be at a scale similar to the flows. However, any similarity in scale does not prove that the features are flows, but does provide circumstantial evidence that they could be.

For the Ginsburg mud volcano, seven clearly identifiable rings are present with radii of between 480 m and 580 m and at heights on the flanks of the volcano of between 125 m and 219 m. From their acoustic shadow lengths (Fig. 2a,b), an average individual flow thickness of 1.3 ± 1 m is estimated. For the Yuma mud volcano, six rings are visible between 420 m and 515 m in radius. Again, similar individual ring amplitudes of about 1.6 ± 1 m are estimated. Eq. 7 yields a volume flux (Q) for flows erupted at an average height of 172 m on the volcano's flank (assuming a calculated conduit radius of 9.4 m). Substituting the estimate of Q into Eq. 9 yields a flow thickness of 2.5 ± 1.3 m, at a height on the flanks of the volcano of about 172 m. Thus both the modelled thickness of the flows and the observed amplitude for the concentric ring structures are within error of one another. Although this does not prove the origin of the rings, it leaves open the possibility that they could

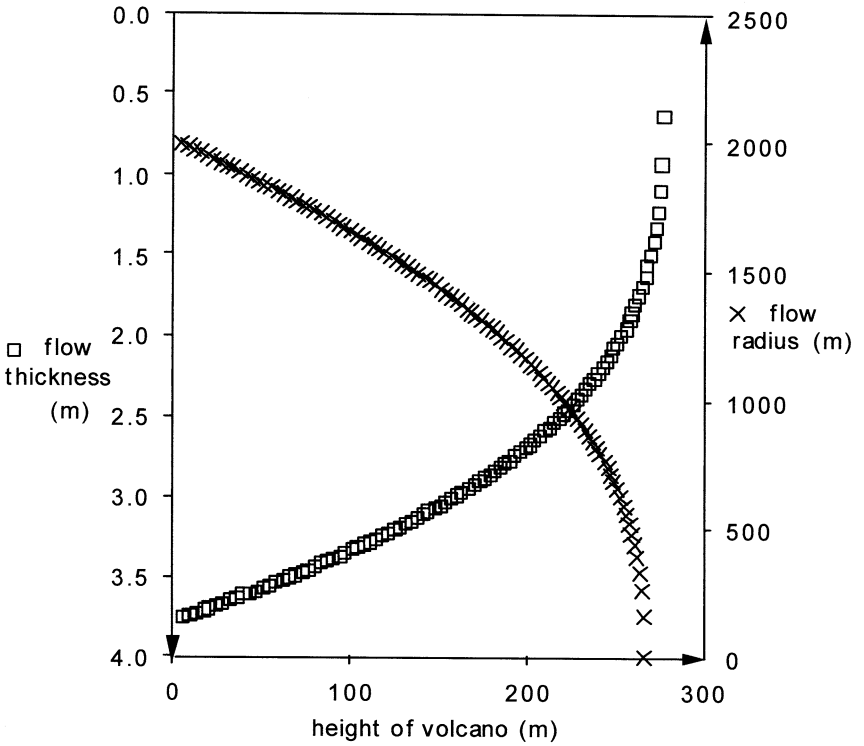

Fig. 6. Results of modelling individual mud flow thickness and radius with height of the volcano, using the isostatic equilibrium model to derive the driving force for eruption and a viscous gravity current flow model for each mud flow. The flow thickness decreases because, as the volcano height increases, the driving force decreases resulting in a lower volume flux for the erupted mud breccia. Similarly, the flow radius decreases, as the volcano height increases, as a result of a lower volume flux and hence lower spreading rate for the erupted mud breccia.

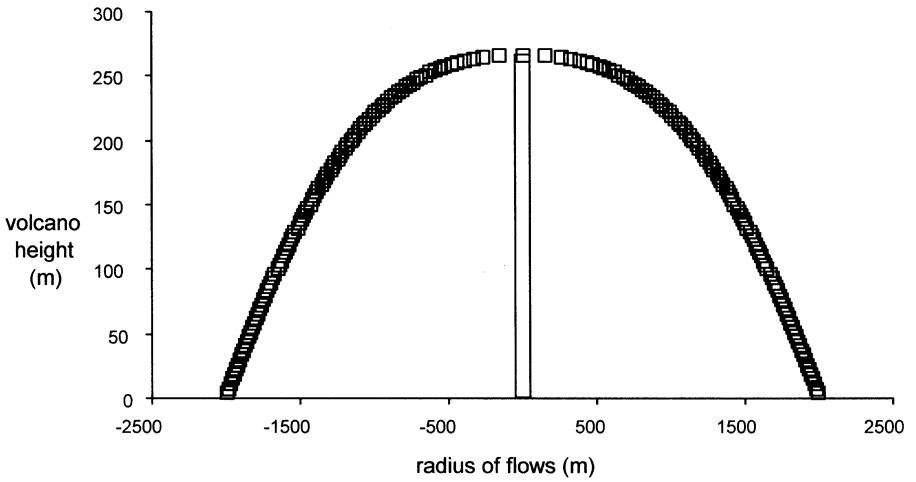

Fig. 7. Results of modelling superimposed mud flows of decreasing radii and thickness with height, using the same parameters as for Fig. 6. The accumulated flows result in a volcano with convex outwards shaped flanks and a gently sloping summit dome. This shape roughly matches that shown by the profiles of the conical mud volcanoes Ginsburg and Yuma (Fig. 2). Although this profile is modelled for starting conditions derived for Yuma and Ginsburg, the general shape of the profile is generic and simply reflects the function of the form of the model.

be the fronts of circular flows as predicted by the model.

3.3.2. *Revised estimates for inertially dominated flow and the consequences of decreasing exit velocity*

The calculated estimates for conduit radii, driving pressure and mud breccia volume flux can now be used to re-assess the preliminary values of t_i, the duration of the initial, inertially dominated flow regime. Estimates of volume flux of between 0.2 m^3 s^{-1} and 470 m^3 s^{-1} have been derived from the model which, when substituted into Eq. 6, give values of t_i of 0.25 s and 12 s respectively. By comparison with the calculated individual flow duration of about 7 h, t_i is negligible, consistent with our initial assumption.

The data from the mud volcano Ginsburg indicate an initial volume flux of 470 m^3 s^{-1} at the base of the volcano (i.e. at the moment the first mud flows started erupting). Since the volume flux (Q) and exit velocity (v_e) are linked only by the conduit area (A), these figures can be used to determine the vertical velocity of the mud breccia as it exits the top of the conduit, e.g.:

$$Q = v_e A \quad (11)$$

$$v_e = Q/\pi r^2 \quad (12)$$

Using the calculated conduit radius (r) of 9.4 m yields a value for the vertical ascent rate (v_e) of mud breccia during its initial eruption at the base of the volcano of 1.6 m s^{-1}. This value decreases to 6×10^{-4} m s^{-1} for eruptions at the summit, where volume fluxes are calculated to be as little as 0.2 m^3 s^{-1}. A potential consequence of this decrease in ascent rate is a tendency for the mud breccia to fractionate, with larger lithoclasts within the mud being too heavy to be ejected by the slow-moving mud, leading to clogging of the conduit. This will result in eruptions from the summit of mature mud volcanoes, that are near to their maximum height of construction, to be fluid-rich while the oldest flows, erupted initially in the volcano's history and now found near the base, will contain large lithoclasts. These predictions are easily testable using long piston coring and drilling provided sufficient depths of penetration are achievable. Alternatively, high-resolution sub-bottom acoustic profile data may be able to resolve the internal structure of the volcanoes, discriminating flow thickness variation and flow superposition sequences.

4. Conclusions

Mud volcanoes are common in ocean settings globally and are probably the result of a variety of tectonic and sedimentary processes. Using numerical modelling can gain insight into their formation by reducing their physical processes to a number of dominant parameters that describe the maximum height of a mud volcano, the thickness and radii of individual flows, and the duration and volume flux for each eruption. Together, these processes are responsible for the first-order shape of the mud volcano. Here, a model is developed for the formation of conical-shaped mud volcanoes, based on buoyancy-driven, viscously retarded gravity flows. The simple modelling of these primary physical processes allows a prediction to be made of the depth to the mud source, as well as determinations of the flux of material erupted. Minimum constraints can be placed on the duration of mud flow eruptions and hence on the construction time of the volcano itself. Importantly, modelling allows an understanding of the key parameters that control mud volcano evolution. Where different morphologies are encountered, whether they are in the same mud volcano or between different volcanoes, the model indicates which physical conditions are dominant in causing these changes.

Results from the modelling, applied to 260 m high, conical-shaped mud volcanoes in the Gulf of Cadiz, predict their formation from about 100 individual flows in which the outermost are the oldest and thickest, and successively higher flows are younger and thinner. Using a model for viscous gravity currents, individual eruptions are predicted to last up to 7 h in duration. The conduit for the mud breccia is calculated to be about 9 m in radius and 4100–4600 m long. The vertical ascent velocity through the conduit decreases as the volcano grows in height, from a maximum of 1.6 m s^{-1} during eruption of the flows forming the base of the volcano to 0.2 m s^{-1} at the summit. As a result, the uppermost flows, erupted as the volcano reaches its maximum elevation, are predicted to be clast-poor and fluid-rich mud, while those erupted rapidly near the base should contain larger and more abundant lithoclasts. Our predictions for the internal structure and evolution of mud volcanoes, and the variation in fluid and clast content of flows, could be tested by coring, drilling and sub-bottom acoustic and seismic profiling.

Acknowledgements

We are indebted to Michael Ivanov, Neil Kenyon, Joan Gardner and José Monteiro for helpful discussions concerning the nature of submarine mud volcanism and on specific aspects of this work. Also to the officers and crew of the R/V *Professor Logachev* without whom none of the data discussed here would be available. We would also like to thank the reviewers (Norman Sleep, Peter Vogt and one anonymous) for their helpful suggestions towards improving this contribution. During the work, J.B. was supported by a Southampton Oceanography Centre, Summer School scholarship. B.M. is supported by the Natural Environment Research Council at Southampton Oceanography Centre.

References

Akhmanov, G., Akhmetzhanov, A., Stadnitskaya, A., Kozlova, E., Mazurenka, L., Teixeira, F., Sautkin, A., Dixon, D., Ovsyannikov, D., Sadekov, A., Rasul, N., Belenkaya, I., Volakova, Yu., Suslova, E., Goncharov, D., 2000. Mud diapirism and mud volcanism study: gulf of Cadiz/Moroccan margin. In: Kenyon: N.H., Ivanov, M.K., Akhmetzhanov, A.M., Akhmanov, G.C. (Eds.), Multidisciplinary Study of the Geological Processes on the North East Atlantic and Western Mediterranean Margins. IOC Technical Series 56, UNESCO, pp. 67–71.

Blankenship, C.L., 1992. Structure and palaeogeography of the External betic Cordillera, southern Spain. Mar. Pet. Geol. 9, 256–264.

Cronin, B.T., Ivanov, M.K., Limonov, A.F., Egorov, A., Akhmanov, G.G., Akhmetjanov, A.M., Kozlova, E., 1997. New discoveries of mud volcanoes on the eastern Mediterranean Ridge. J. Geol. Soc. London 154, 173–182.

Dewey, J.F., Helman, M.L., Turco, E., Hutton, D.H.W., Knott, S.D., 1989. Kinematics of the Western Mediterranean. In: Coward, M. (Ed.), Alpine Tectonics. Spec. Publ. Geol. Soc. London 45, 265–283.

Didden, N., Maxworthy, T., 1982. The viscous spreading of plane and axisymmetric gravity currents. J. Fluid Mech. 121, 27–42.

Flynch, J.A., Bally, A.W., Wu, S., 1996. Emplacement of a passive-margin evaporitic alochthon in the Betic Cordillera of Spain. Geology 24, 67–70.

Gardner, J.M., 2000. Gulf of Cadiz/Moroccan margin, a mud diapirism and mud volcanism study. In: Kenyon, N.H., Ivanov, M.K., Akhmetzhanov, A.M., Akhmanov, G.C. (Eds.), Multidisciplinary Study of the Geological Processes on the North East Atlantic and Western Mediterranean Margins. IOC Technical Series 56, UNESCO, pp. 56–67.

Gardner, J.M., 2001. Mud volcanoes revealed and sampled on the Western Moroccan continental margin. Geophys. Res. Lett. 28, 339–342.

Hovland, M., Hill, A., Stokes, D., 1997. The structure and geomorphology of the Dashgil mud volcano, Azerbaijan. Geomorphology 21, 1–15.

Karig, D.E., 1986. Physical properties and mechanical state of accreted sediments in the Nankai Trough, S.W. Japan. In: Moore, J.C. (Ed.), Structural Fabrics in Deep Sea Drilling Project Cores from Forearcs. Mem. Geol. Soc. Am. 66, 117–133.

Kenyon, N.H., Ivanov, M.K., Akhmetzhanov, A.M., Akhmanov, G.C. (Eds.), 2000. Multidisplinary Study of the Geological Processes on the North East Atlantic and Western Mediterranean Margins. IOC Technical Series 56, UNESCO, 101 pp. plus figures.

Lance, S., Henry, P., Le Pichon, X., Lallemant, S., Chamley, H., Rostek, F., Faugeres, J.C., Gonthier, E., Olu, K., 1998. Submersible study of mud volcanoes seaward of the Barbados accretionary wedge sedimentology, structure and rheology. Mar. Geol. 145, 255–292.

Limonov, A.F., van Weering, T.C.E., Kenyon, N.H., Ivanov, M.K., Meisner, L.B., 1997. Seabed morphology and gas venting in the Black Sea mud volcano area: Observations with the MAK-1 deep-tow side-scan sonar and bottom profiler. Mar. Geol. 137, 121–136.

Maldonado, A., Comas, M.C., 1992. Geology and geophysics of the Alboran Sea: An introduction. Geo-Mar. Lett. 12, 61–65.

Maldonado, A., Somoza, L., 1997. Al zona de fractura Azores-Gibraltar y las cadenas beticas en el Golfo de Cadiz. Evolucion Geologica. 2nd Congress Margen Continental Iberico Atlantico, Abstract. University of Cadiz, Cadiz, pp. 71–72.

Maldonado, A., Somoza, L., Pallarés, L., 1999. The Betic orogen and the Iberian-African plate boundary in the Gulf of Cadiz; geological evolution (central North Atlantic). Mar. Geol. 155, 9–43.

Mascle, A., Moore, J.C., Taylor, E. et al., 1988. Proc. ODP Init. Rep. 110.

Milkov, A.V., 2000. Worldwide distribution of submarine mud volcanoes and associated gas hydrates. Mar. Geol. 167, 29–42.

Rodero, J., Pallerés, L., Maldonado, A., 1999. Late Quaternary seismic facies of the Gulf of Cadiz Spanish continental margin: depositional processes influenced by sealevel changes and tectonic controls. Mar. Geol. 155, 13–56.

Sadekov, A.Y., Ovsyannikov, D.O., 2000. Age of rock clasts from the Yuma and mud volcano breccia on the basis of foraminiferal study (Gulf of Cadiz, NE Atlantic). In: Geological Processes on European Continental Margins (TTR-9 Post-Cruise Conference), Abstracts. University of Granada, Granada.

Shipley, T., Ogawa, Y., Blum, P. et al., 1995. Proc. ODP Init. Rep. 156.

Smith, D.K., Cann, J.R., 1993. Building the crust at the Mid-Atlantic Ridge. Nature 365, 707–715.

Srivastava, S.P., Schouten, H., Roest, W.R., Klitgord, K.D., Kovacs, L.C., Veroef, J., Macnab, R., 1990. Iberian plate kinematics; a jumping plate boundary between Eurasia and Africa. Nature 344, 756–759.

Vogt, P.R., 1974. Volcano height and plate tectonics. Earth Planet. Sci. Lett. 23, 337–348.

Wilson, R.C.L., Hiscott, R.N., Willis, M.G., Gradstein, E.M., 1989. The Lusitanian basin of West-Central Portugal: Mesozoic and Tertiary tectonic, stratigraphic, and subsidence history. In: Tanard, A.J., Balkwill, H.R. (Eds.), Extensional Tectonics and Stratigraphy of the North Atlantic Margins. AAPG Mem. 46, 341–361.